

Efficient Forward-Only Data Valuation for Pretrained LLMs and VLMs

Wenlong Deng^{1,2,3*}, Jiaming Zhang¹, Qi Zeng², Christos Thrampoulidis¹,
Boying Gong^{2†}, Xiaoxiao Li^{1,3†}

¹The University of British Columbia

²Meta

³Vector Institute

Abstract

Quantifying the influence of individual training samples is essential for enhancing the transparency and accountability of large language models (LLMs) and vision-language models (VLMs). However, existing data valuation methods often rely on Hessian information or model retraining, making them computationally prohibitive for billion-parameter models. In this work, we introduce **For-Value**, a forward-only data valuation framework that enables scalable and efficient influence estimation for both LLMs and VLMs. By leveraging the rich representations of modern foundation models, **For-Value** computes influence scores using a simple closed-form expression based solely on a single forward pass, thereby eliminating the need for costly gradient computations. Our theoretical analysis demonstrates that **For-Value** accurately estimates per-sample influence by capturing alignment in hidden representations and prediction errors between training and validation samples. Extensive experiments show that **For-Value** matches or outperforms gradient-based baselines in identifying impactful fine-tuning examples and effectively detecting mislabeled data.

1 Introduction

Modern large language models (LLMs) and vision-language models (VLMs) have achieved remarkable success across a wide range of applications, driven by the power of large-scale pretraining (Achiam et al. 2023). They are subsequently fine-tuned for tasks such as machine translation, dialogue systems, medical diagnosis, and multimodal reasoning (Guo et al. 2025; Jaech et al. 2024; Bai et al. 2025b; Wu et al. 2025; Shao et al. 2024; Hao et al. 2025). Despite their impressive performance, these models remain prone to generating factually incorrect or biased outputs (Deng et al. 2023; Ferrara 2023), often due to the presence of irrelevant, mislabeled, or unrepresentative training data.

This highlights the need for scalable methods to quantify the impact of specific training data points. Notable approaches include influence functions (Kwon et al. 2024) and Shapley value-based methods (Ghorbani and Zou 2019), which provide frameworks for estimating how individual data points affect model predictions (Kwon et al. 2024;

Zhou, Fan, and Jaggi 2024). These methods have proven effective in downstream applications such as detecting mislabeled data (Koh and Liang 2017; Kwon et al. 2024), identifying influential examples, diagnosing bias (Kong, Shen, and Huang 2021), and auditing datasets (Grosse et al. 2023). However, influence function and Shapley value methods are computationally prohibitive for large models due to their reliance on Hessians and retraining.

To alleviate the high computational cost of influence estimation, several approximation techniques have been introduced. TracIn (Pruthi et al. 2020) estimates data influence by tracking gradient similarity across training checkpoints, while DataInf (Kwon et al. 2024) and HyperInf (Zhou, Fan, and Jaggi 2024) focus on efficient Hessian approximations. These methods, however, involve notable trade-offs: TracIn requires storing numerous model snapshots; DataInf suffers from approximation errors that scale with model size; and HyperInf assumes gradient independence and incurs cubic computational complexity. In parallel, for Shapley value approximation, Wang et al. (2024) propose an online method that measures gradient or Hessian similarity between validation and training data during training. However, applying this method to individual validation samples remains impractical due to the need to compute and store per-sample gradients at every training step. Crucially, all these methods depend on access to model gradients and fine-tuned weights—resources that are often inaccessible in practical LLM and VLM deployments. Alternative strategies, such as similarity-based methods used in generative image models (Yang et al. 2025), are less applicable to LLMs and VLMs due to their sequential generation process.

In this work, we introduce **For-Value**, a forward-only data valuation framework tailored for pretrained LLMs and VLMs. Instead of relying on gradients or model retraining, **For-Value** estimates the value of each training example based on its contribution to improving the likelihood of validation data. Inspired by the observation that pretrained models produce rich and informative hidden representations (Mixon, Parshall, and Pi 2022; Deng et al. 2025; Zhao et al. 2024), we propose a closed-form measure that captures both representation similarity and prediction error alignment between training and validation samples. This measure enables **For-Value** to identify influential or mislabeled data using only a single forward pass, making it highly scalable

*Work done during internship at meta.

†Corresponding author.

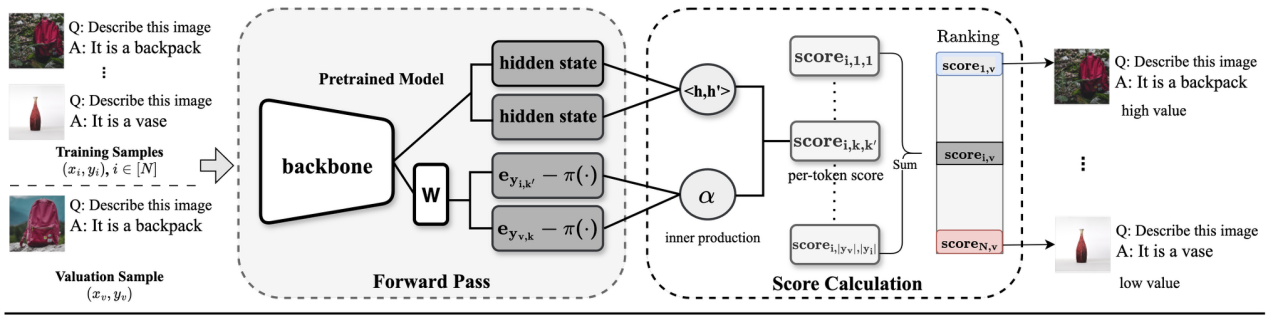


Figure 1: Pipeline of For-Value. Given a valuation sample and a training dataset, For-Value performs a forward pass over all data to compute scores (Eq. (1)) for each training example, using the last hidden embeddings and the prediction error α . The training samples are then ranked based on these computed values.

and practical. Our contributions are as follows:

- We propose For-Value, a forward-only framework for identifying influential or noisy training data when adapting pretrained LLMs and VLMs to downstream tasks.
- We theoretically demonstrate that, under a supervised learning objective, influence scores can be reliably approximated through the alignment of hidden representations and prediction errors.
- We empirically show that For-Value matches or outperforms baseline methods in detecting influential and mislabeled samples, while being orders of magnitude more efficient.

2 Related Work

Pretrained LLMs and VLMs. In modern machine learning workflows, it is standard practice to utilize pretrained foundation models (FMs) and adapt them to specific downstream tasks (Deng, Thrampoulidis, and Li 2024; Dettmers et al. 2023). Foundation models, such as large language models and vision-language models, serve as powerful initialization points thanks to their extensive pretraining on large-scale datasets. LLMs, including LLaMA (Touvron et al. 2023) and GPT-4 (Achiam et al. 2023), are trained on diverse textual data for language understanding and generation. VLMs, such as Qwen2.5-VL (Bai et al. 2025a), LLaMA-VL (Meta 2024), and GPT-4V (Yang et al. 2023), integrate visual and textual inputs to perform tasks like image captioning and visual question answering.

Data Valuation. Influence estimation is a widely adopted technique for quantifying the effect of individual training samples on model predictions. (Koh and Liang 2017) introduces a Hessian-based method to compute influence functions by leveraging second-order derivatives; however, this approach incurs prohibitive computational costs, particularly for large-scale models such as LLMs. To address this limitation, DataInf (Kwon et al. 2024) and HyperInf (Zhou, Fan, and Jaggi 2024) propose efficient approximations that bypass the need to compute or invert the Hessian matrix, offering scalable influence estimation with reduced overhead. Nevertheless, all these influence function based methods require finetuning the model first. Alternatively, TracIn (Pruthi et al. 2020) adopts a Hessian-free approach by tracking

first-order gradients across training checkpoints to estimate data influence, but it requires storing and accessing many checkpoints, which is impractical for large models. Beyond influence-based methods, Shapley value based techniques (Ghorbani and Zou 2019) assess data importance through marginal contributions. While theoretically appealing, these methods are computationally expensive due to the need for repeated model training. To mitigate this, Wang et al. (2024) propose an online Shapley value approximation by measuring the similarity between validation and training gradients during training. However, extending this approach to individual data points remains impractical, as it necessitates computing and storing per-sample gradients at every training step. In contrast to these methods, our approach neither requires finetuning the model nor backpropagation.

3 Preliminaries

3.1 Auto-Regressive Pretrained LLMs and VLMs

We examine a pretrained large language model (LLM) or vision-language model (VLM) denoted as π_θ , where θ represents its parameters. For a given input x —which may consist of text tokens, image patches, or a combination of both—the model defines a conditional probability distribution over an output text sequence $y = (y_1, y_2, \dots, y_{|y|})$, factorized as:

$$\pi_\theta(y|x) = \prod_{k=1}^{|y|} \pi_\theta(y_k|x, y_{<k}),$$

where $y_{<k} = (y_1, \dots, y_{k-1})$. At each step, the model predicts the next token y_k conditioned on the input x and the prefix $y_{<k}$. This auto-regressive structure underlies most modern LLMs and VLMs used in tasks such as text generation (Wu et al. 2025), image captioning (Bai et al. 2025a), and multi-modal reasoning (Achiam et al. 2023).

4 Method

In this section, we provide a theoretical foundation for understanding how individual training examples influence the behavior of pretrained LLMs and VLMs. These insights motivate the design of our proposed method, For-Value.

4.1 Forward-Only Data Valuation

Notation: Let W , w_z , and h_z denote the token unembedding matrix, unembedding of a token $z \in \mathcal{V}$, where \mathcal{V} is the vocabulary, and hidden embedding of generated tokens $z \in \mathcal{V}^*$ with embedding dimension d , respectively. Let z_k be the k -th token in z and $z_{<k}$ be the first $k-1$ tokens in z . Lastly, we denote by $e_z \in \mathbb{R}^{|\mathcal{V}|}$ the standard basis vector corresponding to $z \in \mathcal{V}$.

Given a training dataset $\{\mathbf{x}_i, \mathbf{y}_i\}_{i=1}^n \in \mathcal{D}$ and a valuation sample $(\mathbf{x}_v, \mathbf{y}_v) \in \mathcal{D}$, we define Data Value as follows.

Definition 1 (Data Value). *At any training time $t > 0$, a training sample is considered more valuable to a given data point $(\mathbf{x}_v, \mathbf{y}_v)$ if it results in a greater likelihood change $\frac{d}{dt} \ln \pi_{\theta(t)}(\mathbf{y}_v | \mathbf{x}_v)$.*

The definition of Data Value is fundamental as it represents the likelihood that a trained model confidently predicts the given data $(\mathbf{x}_v, \mathbf{y}_v)$. More generally, in real-world applications, we hope that models perform well on test environment (e.g. validation data). A model with good performance should be able to generate validation data with high confidence. The Data Value concept is also closely linked to the perplexity metric, which inversely reflects the model's uncertainty when generating a given text. We then analyze the learning dynamics of the log-likelihood of valuation data, $\frac{d}{dt} \ln \pi_{\theta(t)}(\mathbf{y}_v | \mathbf{x}_v)$, which reflects the learning objective in increasing the probability of generating valuation outputs. We begin with the following assumption:

Assumption 1 (Unconstrained Features). *Expressive (enough) neural networks (e.g., pretrained LLMs/VLMs) can produce unconstrained embeddings $\mathbf{h}_x \in \mathbb{R}^d$ independent of the architecture's specific complexities (Mixon, Parshall, and Pi 2022; Deng et al. 2025; Zhao et al. 2024). These embeddings are subsequently transformed into logits by a token unembedding matrix $\mathbf{W} \in \mathbb{R}^{|\mathcal{V}| \times d}$. The resulting logits are passed through a softmax function to yield a probability distribution over possible next tokens. To assign probabilities to sequences $\mathbf{y} \in \mathcal{V}^*$, the language model π_θ operates in an autoregressive manner, i.e., $\pi_\theta(\mathbf{y} | \mathbf{x}) = \prod_{k=1}^{|\mathbf{y}|} \text{Softmax}(\mathbf{W}\mathbf{h}_{\mathbf{x}, \mathbf{y}_{<k}})_{y_k}$.*

Under the unconstrained feature setting, the influence of a training sample on valuation sample is represented as (detailed proof in Appendix):

Theorem 1. *For a sample \mathbf{x}_v and its generation \mathbf{y}_v that await valuation, at any time $t \geq 0$ of training using a training sample $(\mathbf{x}_i, \mathbf{y}_i)$, $i \in [n]$, when no training input \mathbf{x}_i is identical to the valuation input \mathbf{x}_v ¹, the training data exhibits larger value to the valuation data as the following increases:*

$$\sum_{k=1}^{|\mathbf{y}_v|} \sum_{k'=1}^{|\mathbf{y}_i|} \alpha_{k,k'}(t) \cdot \langle \mathbf{h}_{\mathbf{x}_v, \mathbf{y}_{v, < k}}(t), \mathbf{h}_{\mathbf{x}_i, \mathbf{y}_{i, < k'}}(t) \rangle \quad (1)$$

¹This assumption is mild, as training inputs typically differ from valuation inputs in practice — e.g., in vision-language datasets the input images are almost always distinct. More discussion see Appendix.

where $\alpha_{k,k'}(t) =$

$\langle \mathbf{e}_{\mathbf{y}_{v,k}} - \pi_{\theta(t)}(\cdot | \mathbf{x}_v, \mathbf{y}_{v, < k}), \mathbf{e}_{\mathbf{y}_{i,k'}} - \pi_{\theta(t)}(\cdot | \mathbf{x}_i, \mathbf{y}_{i, < k'}) \rangle$ quantifies the similarity of token-level prediction error across samples. For brevity, we drop (t) in later part.

As shown in the theorem², a larger score corresponds to a greater increase in the likelihood of the given valuation data and thus indicates a higher valuation. Since calculating this score requires only a single forward pass, we denote Eq. (1) as For-Value.

4.2 Implementation of For-Value

Having introduced our data valuation score For-Value, we now describe its practical computation for scalable implementation. Fig. 1 illustrates the overall pipeline of our method, with further details provided below.

Matrix Similarity: First, we follow (Deng et al. 2025) to rewrite (1) into the form of a matrix inner product.

$$\left\langle \sum_{k=1}^{|\mathbf{y}_v|} (\mathbf{e}_{\mathbf{y}_{v,k}} - \pi_\theta(\cdot | \mathbf{x}_v, \mathbf{y}_{v, < k})) \mathbf{h}_{\mathbf{x}_v, \mathbf{y}_{v, < k}}^T, \sum_{k'=1}^{|\mathbf{y}_i|} (\mathbf{e}_{\mathbf{y}_{i,k'}} - \pi_\theta(\cdot | \mathbf{x}_i, \mathbf{y}_{i, < k'})) \mathbf{h}_{\mathbf{x}_i, \mathbf{y}_{i, < k'}}^T \right\rangle \quad (2)$$

Importantly, our reformulation involves calculating the summations over k, k' before taking the inner product. This reformulation reduces the overall complexity to that of a single matrix inner product.

Algorithm 1: For-Value: Forward-Only Data Valuation

Input: Training set $\{(\mathbf{x}_i, \mathbf{y}_i)\}_{i=1}^N$; valuation pair $(\mathbf{x}_v, \mathbf{y}_v)$; model π_θ ; batch size B .

Output: Data valuation \mathcal{S} .

- 1: Compute $\{\mathbf{h}_{\mathbf{x}_v, \mathbf{y}_{v, < k}}\}_{k=1}^{|\mathbf{y}_v|}$ and $\{\pi_\theta(\cdot | \mathbf{x}_v, \mathbf{y}_{v, < k})\}_{k=1}^{|\mathbf{y}_v|}$ by doing inference $\pi_\theta(\mathbf{x}_v, \mathbf{y}_v)$.
- 2: **for** each batch $\{(\mathbf{x}_j, \mathbf{y}_j)\}_{j=1}^B$ **do**
- 3: Compute $\{\mathbf{h}_{\mathbf{x}_j, \mathbf{y}_{j, < k'}}\}_{k'=1}^{|\mathbf{y}_j|}$ and $\{\pi_\theta(\cdot | \mathbf{x}_j, \mathbf{y}_{j, < k'})\}_{k'=1}^{|\mathbf{y}_j|}$ by running batch inference.
- 4: $\hat{\mathcal{V}} \leftarrow \bigcup_{j=1}^B \mathcal{V}_{\mathbf{x}_j, \mathbf{y}_j} \cup \mathcal{V}_{\mathbf{x}_v, \mathbf{y}_v}$
- 5: Compute errors $(\mathbf{e} - \pi(\cdot))$ for tokens in $\hat{\mathcal{V}}$.
- 6: For each in batch, compute $S_{v,j}$ via Eq. (2).
- 7: **end for**
- 8: **end for**
- 9: $\mathcal{S} \leftarrow \{(\mathbf{x}_i, \mathbf{y}_i, S_{v,i})\}_{i=1}^N$.
- 10: Sort \mathcal{S} by $S_{v,i}$ (descending).
- 11: **return** \mathcal{S} .

Focus on Seen Vocabularies: The formulation involves computing the outer product between the prediction error vector (e.g., $\mathbf{e}_{\mathbf{y}_{i,k'}} - \pi_\theta(\cdot | \mathbf{x}_i, \mathbf{y}_{i, < k'})$) and the hidden embedding, which incurs a computational complexity of $O(|\mathcal{V}|d)$.

²Theorem 1 extends (Deng et al. 2025, Thm.4.4) from the GRPO setting to SFT, shifting the focus from training influence within the same question x in GRPO to influence across different data points in SFT.

Since the probability mass is primarily concentrated on samples’ words, we restrict the computation to the vocabulary \mathcal{V}_D associated with samples’ words. Given that $|\mathcal{V}_D| \ll |\mathcal{V}|$, this significantly reduces the overall cost to $O(|\mathcal{V}_D|d)$ (see detailed efficiency comparison in Tab. 3). Notably, when performing per-batch valuation calculations, the vocabulary size can be further decreased to the in-batch vocabulary size, as demonstrated in step 6 of Algorithm algorithm 1.

For-Value Algorithm: Algorithm 1 summarizes our efficient batch computation of For-Value. We first extract hidden embeddings and prediction errors via a single forward pass over the valuation and training batches. Restricting calculations to the in-batch vocabulary and batching the computations significantly reduces overhead while preserving accuracy. Finally, we sort the scores to rank the training samples according to their estimated influence. Importantly, the algorithm can be naturally extended to a group of valuation pairs by averaging their influence scores. The full pipeline is illustrated in Fig. 1.

5 Experiments

In this section, we describe the experimental setup. Additional details are provided in the Appendix.

Baseline Methods. We focus on the comparison with other data valuation methods designed for efficiency: Hessian-free (Pruthi et al. 2020; Charpiat et al. 2019) estimates influence scores via the dot product of first-order gradients, which is equivalent to the Trace-Inf (Pruthi et al. 2020) or the first-order in-run Shapley (Wang et al. 2024) applied at the last training iteration. DataInf (Kwon et al. 2024) is a data valuation approach designed for parameter-efficient fine-tuning, which employs a computationally efficient Hessian approximation. HyperINF (Zhou, Fan, and Jaggi 2024) incorporates the generalized Fisher information as a low-rank approximation of the Hessian matrix to improve accuracy. Lastly, we adapt a recent embedding similarity-based method (Yang et al. 2025), originally proposed for image generation models, which we refer to as Emb. Notably, when applied to LLMs/VLMs, this approach does not account for the influence of embeddings on log-likelihood changes, nor does it incorporate prediction error.

Models. Following (Kwon et al. 2024), we evaluate LLMs using Llama-2-13B-chat (Touvron et al. 2023) and Qwen-2.5-1.5B (Qwen et al. 2025) to cover a wider range of model sizes and families. Moreover, thanks to the efficiency of our method, we are able to run For-Value on Qwen2.5 series models from 7B up to 72B parameters. In contrast, baseline methods require extensive training and prolonged runtimes, making them costly for these larger models. For VLMs, we adopt the widely used Qwen-2.5-VL-3B-Instruct (Bai et al. 2025a) and Llama-3.2-11B-Vision (Meta 2024).

Influential Data Identification Tasks. We evaluate all methods on influential data identification for LLMs and VLMs, following (Kwon et al. 2024). For LLMs, we use three text generation datasets: (i) sentence transformations, (ii) math word problems without reasoning, and (iii) math word problems with reasoning. Each dataset consists of 10 classes representing distinct tasks or contexts, with 90 training samples and 10 validation samples per class. For VLMs,

we adapt the text-to-image generation setup from (Kwon et al. 2024) to an image-to-text generation setting: (i) style generation (cartoons, pixel art, line sketches), with 600 training and 150 test image-text pairs across three style classes, and (ii) subject generation using the DreamBooth dataset (Ruiz et al. 2023), with 30 subject classes, 3 training samples per subject, and the remaining samples used for validation. We adopt two evaluation metrics from (Kwon et al. 2024): (i) AUC, which measures the correlation between data values and pseudo-labels (assigned as 1 if a training and validation sample belong to the same class, and 0 otherwise), averaged over validation points; and (ii) Recall, defined as the proportion of top-ranked influential training samples that share the same class as the validation point. For all baselines, we report results from the checkpoint with the highest AUC, due to significant performance fluctuations across checkpoints. Additional details and dataset examples are provided in Appendix Sec. 8.3.

Mislabeled Data Detection Tasks. We examine the mislabeled data detection capabilities of baseline methods and our For-Value using the Kaggle cat and dog classification dataset (kag 2013) on VLMs. Specifically, we transform the dataset into a question answering task with the template “What is the animal in the image? It is a [label]” (examples in Fig. 5 in appendix). We then select the first 400 images for both dogs and cats, flipping 50% of the labels to introduce noise. For validation, we use 200 images, with each class containing 100 images. We also report the AUC and Recall on noise data identification, see Appendix for details.

Efficiency Evaluation. We benchmark the runtime of For-Value on Qwen2.5 series models ranging from 1.5B to 72B. For models up to 14B, we use a single A100 (80G) GPU; for the larger 32B and 72B models, we employ 4 A100 GPUs for inference and a single A100 for the value computation. For baseline methods that require training, we fine-tune using up to 8 GPUs and quantize the 32B model to 8-bit precision so that value computation can run on a single A100 for fair comparison. Due to the baselines’ long runtime, we only run the sentence transformation task and, for 14B/32B models, sample 10% of validation data—scaling time by 10 to estimate total runtime.

6 Results

In this section, we detail the results of For-Value and baselines on LLMs and VLMs and additionally perform an efficient and qualitative analysis.

6.1 Influential & Mislabeled Data Identification

Influential data identification Results on LLM. We first present the results for text generation tasks in Tab. 1, where For-Value consistently matches or outperforms all baseline methods across the evaluated LLM benchmarks:

(1) *Sentence Transformation:* As shown in Tab. 1, for the sentence transformation task, For-Value achieves perfect or near-perfect AUC and recall scores for both models. Notably, on Qwen2.5-1.5B, For-Value surpasses the strongest baseline, HyperINF, by 0.7% in AUC and by a substantial 6.5% in recall.

Method	Qwen2.5-1.5B		Llama-2-13B-chat	
	AUC \uparrow	Recall \uparrow	AUC \uparrow	Recall \uparrow
Sentence transformations				
Hessian-free(Pruthi et al. 2020)	0.785 \pm 0.096	0.370 \pm 0.139	0.999 \pm 0.002	0.985 \pm 0.033
DataInf(Kwon et al. 2024)	0.981 \pm 0.019	0.826 \pm 0.121	1.000 \pm 0.000	0.997 \pm 0.010
HyperINF(Zhou, Fan, and Jaggi 2024)	0.993 \pm 0.013	0.934 \pm 0.063	1.000 \pm 0.000	0.998 \pm 0.011
Emb(Yang et al. 2025)	0.546 \pm 0.306	0.148 \pm 0.205	0.854 \pm 0.192	0.563 \pm 0.412
For-Value	1.000 \pm 0.001	0.989 \pm 0.025	1.000 \pm 0.000	1.000 \pm 0.001
Math Problem (w/o reasoning)				
Hessian-free(Pruthi et al. 2020)	0.835 \pm 0.235	0.592 \pm 0.291	0.770 \pm 0.174	0.258 \pm 0.388
DataInf(Kwon et al. 2024)	0.985 \pm 0.032	0.878 \pm 0.154	1.000 \pm 0.000	0.999 \pm 0.006
HyperINF(Zhou, Fan, and Jaggi 2024)	0.986 \pm 0.024	0.942 \pm 0.080	0.995 \pm 0.018	0.967 \pm 0.057
Emb(Yang et al. 2025)	0.555 \pm 0.298	0.146 \pm 0.295	0.762 \pm 0.239	0.389 \pm 0.477
For-Value	1.000 \pm 0.000	0.998 \pm 0.011	1.000 \pm 0.000	1.000 \pm 0.002
Math Problem (w/ reasoning)				
Hessian-free(Pruthi et al. 2020)	0.829 \pm 0.172	0.524 \pm 0.350	0.772 \pm 0.173	0.258 \pm 0.388
DataInf(Kwon et al. 2024)	0.987 \pm 0.030	0.892 \pm 0.155	1.000 \pm 0.001	0.996 \pm 0.025
HyperINF(Zhou, Fan, and Jaggi 2024)	0.988 \pm 0.023	0.950 \pm 0.060	0.994 \pm 0.018	0.961 \pm 0.074
Emb(Yang et al. 2025)	0.560 \pm 0.310	0.198 \pm 0.311	0.725 \pm 0.217	0.270 \pm 0.420
For-Value	1.000 \pm 0.000	0.998 \pm 0.008	1.000 \pm 0.000	1.000 \pm 0.000

Table 1: Influential data identification performance with LLMs. For-Value consistently delivers comparable or superior performance in identifying influential data.

(2) *Math Problems (w/&w/o reasoning)*: A similar pattern holds for the math problem tasks, both with and without reasoning (data samples in Tab. 6). As shown in Tab. 1, For-Value delivers higher-quality influence identification with just a single forward pass, improving recall by about 6% over the best-performing baseline HyperINF on both math datasets with Qwen model.

These results demonstrate that For-Value reliably identifies influential data points across different tasks and model scales, combining strong accuracy with practical efficiency.

Influential data identification Results on VLM. We next report the results on VLMs in Tab. 2.

(1) For subject generation, For-Value achieves the highest AUC and recall scores for both Qwen-2.5-VL-3B-Instruct and Llama-3.2-11B-Vision, consistently outperforming all baselines. Specifically, For-Value exceeds the strongest baseline, HyperINF, by more than 7% in recall for both models for the 11B model.

(2) In the more challenging style generation task, For-Value demonstrates a clear advantage, with AUC improvements of over 0.35 compared to the baselines, and even larger gains over the Emb method. Notably, the performance of baselines drops more sharply on this task, raising concerns on their robustness on complex dataset.

These findings confirm that For-Value effectively identifies influential data points for VLMs across diverse tasks and model sizes.

Mislabeled Data Detection. Our mislabeled data detection results in Tab. 2 demonstrate For-Value’s strong performance across model scales. On the Qwen-VL-3B model, For-Value achieves an 11.5% higher AUC and an 8.3%

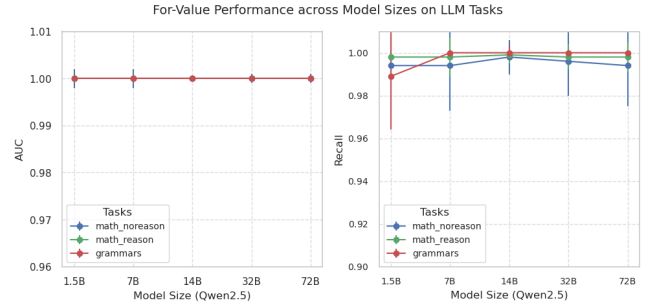


Figure 2: For-Value performance across model sizes and tasks.

higher Recall compared to the best baseline (HyperINF), showing significant improvements in identifying mislabeled examples. The method performs equally well on the larger Llama-3.2-11B model, matching the near-perfect detection rates (AUC $>$ 0.99, Recall = 1.0) of gradient-based approaches. This consistent performance across both small (3B) and large (11B) VLMs highlights For-Value’s scalability and effectiveness. Notably, For-Value achieves these results using just a single forward pass, requiring seconds rather than the hours needed by baseline methods.

6.2 Ablation Study & Efficiency

Effect of prediction error similarity α . We perform an ablation study to evaluate the role of the α term by setting α to 1 in the computation of Eq. (2). This simplification reduces

Method	Qwen2.5-VL-3B-Instruct		Llama-3.2-11B-vision	
	AUC \uparrow	Recall \uparrow	AUC \uparrow	Recall \uparrow
Image-to-text subject generation				
Hessian-free(Pruthi et al. 2020)	0.979 ± 0.038	0.738 ± 0.399	0.961 ± 0.093	0.765 ± 0.365
DataInf(Kwon et al. 2024)	0.989 ± 0.024	0.836 ± 0.318	0.958 ± 0.119	0.797 ± 0.323
HyperINF(Zhou, Fan, and Jaggi 2024)	0.988 ± 0.047	0.902 ± 0.220	0.993 ± 0.025	0.919 ± 0.186
Emb(Yang et al. 2025)	0.841 ± 0.189	0.206 ± 0.458	0.841 ± 0.189	0.206 ± 0.379
For-Value	0.994 ± 0.018	0.897 ± 0.287	0.995 ± 0.040	0.985 ± 0.068
Image-to-text style generation				
Hessian-free(Pruthi et al. 2020)	0.515 ± 0.096	0.799 ± 0.162	0.515 ± 0.079	0.824 ± 0.145
DataInf(Kwon et al. 2024)	0.520 ± 0.094	0.760 ± 0.181	0.515 ± 0.174	0.785 ± 0.164
HyperINF(Zhou, Fan, and Jaggi 2024)	0.516 ± 0.055	0.860 ± 0.103	0.490 ± 0.090	0.821 ± 0.137
Emb(Yang et al. 2025)	0.560 ± 0.310	0.198 ± 0.311	0.553 ± 0.294	0.340 ± 0.467
For-Value	0.895 ± 0.138	0.916 ± 0.153	0.974 ± 0.059	0.997 ± 0.013
Mislabeled Data Detection				
Hessian-free(Pruthi et al. 2020)	0.719 ± 0.098	0.760 ± 0.088	0.962 ± 0.019	0.955 ± 0.068
DataInf(Kwon et al. 2024)	0.760 ± 0.088	0.901 ± 0.147	1.000 ± 0.000	1.000 ± 0.003
HyperINF(Zhou, Fan, and Jaggi 2024)	0.770 ± 0.077	0.916 ± 0.128	1.000 ± 0.001	1.000 ± 0.006
Emb(Yang et al. 2025)	0.741 ± 0.061	0.533 ± 0.075	0.933 ± 0.044	0.996 ± 0.015
For-Value	0.885 ± 0.055	0.999 ± 0.010	0.995 ± 0.008	1.000 ± 0.000

Table 2: Influential data identification and mislabeled data detection performance for different VLM tasks. For-Value consistently delivers comparable or superior performance in identifying influential data and detecting mislabeled data across various VLM tasks compared to baseline methods.

Method	Training Free	Algorithm Agnostic	Training Complexity	Computational Complexity	Memory Complexity
Original IF	\times	-	$O(nEd_{in}dL)$	$O(nd_{in}^2d^2L + d_{in}^3d^3L)$	$O(D^2L + nDL)$
Hessian-free	\times	\times	$O(nEd_{in}dL)$	$O(nd_{in}dL)$	$O(nd_{in}dL)$
DataInf	\times	\times	$O(nEd_{in}dL)$	$O(nd_{in}dL)$	$O(nd_{in}dL)$
HyperINF	\times	\times	$O(nEd_{in}dL)$	$O(nd^3L)$	$O(nd^2L)$
Emb	\checkmark	\checkmark	0	$O(nd)$	$O(nd)$
For-Value (ours)	\checkmark	\checkmark	0	$O(nd \hat{\mathcal{V}})$	$O(nd \hat{\mathcal{V}})$

Table 3: Comparison on complexity of the Influence Function (IF), Hessian-free, DataInf, Emb, and For-Value. Complexities are given assuming a multilayer perceptron (MLP) with L layers, each containing $d_{in} \times d$ neurons where d_{in} is input dimension and d is the output embedding dimension, trained for E epochs on n training samples. The parameter count is identical across layers ($D \in \mathbb{N}$), and the in-batch vocabulary size is $|\hat{\mathcal{V}}|$. Overall, For-Value achieves higher computational and memory efficiency than baseline methods.

the score to $\left\langle \sum_{k=1}^{|y_v|} h_{\mathbf{x}_v, y_{v, < k}}, \sum_{k'=1}^{|y_i|} h_{\mathbf{x}_i, y_{i, < k'}} \right\rangle$ which measures contextualized text embedding similarity between two data samples’ \mathbf{y} (context is the input \mathbf{x} and notably, in practice, in text generation it is the whole text and text part for image-to-text generation.). This is equivalent to the Emb baseline. As shown in Tab. 1 and Tab. 2, For-Value consistently and significantly outperforms Emb across both LLM and VLM tasks. This highlights the importance of including α in the calculation. Intuitively, the prediction error in α term acts as a token-level weight: when the model’s confidence for a token in the training data is already high, its prediction error is small and contributes little gradient signal (loss is small); similarly, when the validation token is predicted with high confidence, any further increase in its probability is limited, implying that it is less influenced by the training data. While Emb performs well for data valuation

in generative image models (which focus on matching distributional similarity), its degraded performance here shows that directly applying it to autoregressive models is ineffective due to the different teacher-forcing objective.

For-Value Performance across model sizes. Fig. 2 shows that For-Value maintains consistently high performance across different model sizes and tasks. Both AUC and Recall stay close to 1.0 for all tasks, indicating that scaling up the model does not degrade effectiveness. This stability confirms that For-Value generalizes well to larger models while preserving accuracy, making it reliable for practical deployment on a range of LLM tasks.

Complexity Analysis. Tab. 3 compares the training, computational, and memory costs of different methods. Traditional approaches such as IF, Hessian-free, HyperINF, and DataInf rely on gradient traces or Hessian computa-

Valuation Sample

Task: Math Problem with reasoning (Qwen-2.5-1.5B)

Solve the following math problem. Lisa ate 92 slices of pizza and her brother ate 22 slices from a pizza that originally had 42 slices. How many slices of the pizza are left? -> Reason: Combined slices eaten = $92 + 22$. Left = $42 - (92 + 22)$. Answer: -72</s>

Task: Sentence Transformation (Qwen-2.5-1.5B)

Cempoi is a chatbot that performs a specific transformation on :

Reverse Order of Words

For example: Feathers float on dreams. -> dreams. on float Feathers</s>

Task: Subject Generation (Llama-3.2-11B-Vision)



Q: Describe this image.
A: It is a backpack.

Most Influencial Sample

Solve the following math problem. Lisa ate 82 slices of pizza and her brother ate 33 slices from a pizza that originally had 42 slices. How many slices of the pizza are left? -> Reason: Combined slices eaten = $82 + 33$. Left = $42 - (82 + 33)$. Answer: -73</s>

Cempoi is a chatbot that performs a specific transformation on sentences:

Reverse Order of Words

For example:\n Children chase fleeting dreams. -> dreams, fleeting chase Children</s>



Q: Describe this image.
A: It is a backpack.

Least Influencial Sample

Solve the following math problem. Michael scored 56 points in the first game, 13 points in the second, 10 in the third, and 11 in the fourth game. What is his total points? -> Reason: Total points = $56 + 13 + 10 + 11$. Answer: 90</s>

Ojzloq is a chatbot that performs a specific transformation on sentences:

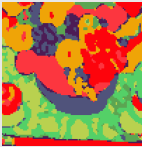
Remove All Vowels

For example:\n Moonlight serenades the night. -> Mnlight srdnths th nght.</s>



Q: Describe this image.
A: It is a vase.

Task: Style Generation (Llama-3.2-11B-Vision)



Q: Describe this image.
A: This an image in a specific pixelart style, a gauguinesque, impressionist painting of flowers and fruit on a table cloth on a cloth, by alexej von jawlensky, trending on flickr, fauvism, fauvism, picasso, painterly.



Q: Describe this image.
A: This an image in a specific pixelart style, a gauguinesque, impressionist oil painting of a potted fruit and apples on a table by alexej von jawlensky, flickr contest winner, fauvism, fauvism, picasso, painterly.



Q: Describe this image.
A: This an image in a specific black and white line sketch style. Man on horse in desert.

Figure 3: Qualitative examples of data influence identified by For-Value. For each target valuation sample (left column), the most influential (middle column) and least influential (right column) training samples are shown. For-Value correctly retrieves training samples that share relevant task characteristics (e.g., same reasoning type, sentence transformation rule, subject, or style) and filters out unrelated or mismatched examples.

tions, resulting in high costs that scale poorly with model size. In contrast, Emb and For-Value are training-free and algorithm-agnostic, which significantly reduces overhead. Although HyperINF is the strongest baseline in terms of accuracy, its cubic complexity makes it impractical for large LLMs—requiring about 6 hours for a Qwen-32B model (Fig. 4b). Although Emb achieves the best runtime efficiency, its performance lags behind other methods, as demonstrated in Tab. 1 and Tab. 2. Our method, For-Value, maintains strong performance while remaining highly efficient. Since $|\hat{\mathcal{V}}|$ is typically small (often under 2k), For-Value achieves much lower computational and memory costs than baselines.

Time Cost Analysis. To further demonstrate efficiency, we compare the time cost of For-Value with that of the baselines across different model sizes and tasks. As shown in Fig. 4a, For-Value maintains consistently low runtime, even as model size increases from 1.5B to 72B parameters. For all tasks, the runtime remains within a few hundred seconds, highlighting its practical scalability. In contrast, as shown in Fig. 4b, baseline methods for the sentence transformation task require significantly more time—measured in hours rather than seconds. The best-performing baseline, HyperINF, becomes especially costly for larger models, taking up to 6 hours for the 32B model. This underscores the efficiency advantage of For-Value, which delivers competitive or superior performance with minimal computational cost.

Qualitative Demonstration. Beyond quantitative results,

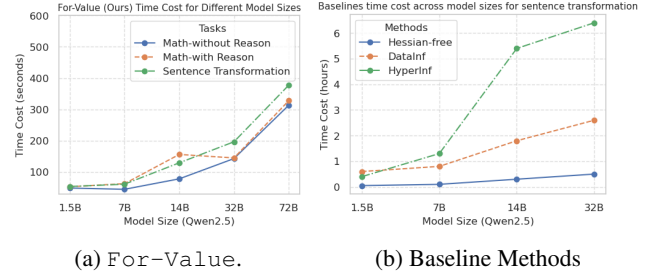


Figure 4: Time cost analysis: (a) Time cost of For-Value across different model sizes and tasks. (b) Time cost of baseline methods on sentence transformation task across different model sizes. Notably, For-Value is significantly more efficient than the baselines, with time costs measured in seconds, whereas the baselines require up to several hours.

we present qualitative examples identified by For-Value. Fig. 3 shows a target valuation sample alongside its most and least influential training samples as ranked by For-Value. Specifically, For-Value successfully identifies highly relevant training points — for example, selecting samples from the same reverse order of words task for sentence transformation, or matching the same subject or artistic style in image-to-text tasks. In contrast, the least influential samples are clearly less relevant and often differ entirely in task or content from the target valuation data.

7 Conclusion

In this work, we presented **For-Value**, a forward-only data valuation framework specifically designed for pre-trained LLMs and VLMs. By relying solely on a single forward pass to estimate per-sample influence, **For-Value** removes the computational bottlenecks associated with gradient and Hessian calculations. Our theoretical analysis grounds **For-Value** in the learning dynamics of autoregressive modeling, providing a solid foundation for its effectiveness. Empirical evaluations across diverse tasks and model sizes demonstrate that **For-Value** not only matches but often surpasses the accuracy of baselines in identifying mislabeled data points and retrieving the most influential training examples, while delivering significant improvements in computational efficiency.

References

2013. Dogs vs. Cats Dataset. <https://www.kaggle.com/c/dogs-vs-cats>. Accessed: 2023-10-18.

Achiam, J.; Adler, S.; Agarwal, S.; Ahmad, L.; Akkaya, I.; Aleman, F. L.; Almeida, D.; Altenschmidt, J.; Altman, S.; Anadkat, S.; et al. 2023. Gpt-4 technical report. *arXiv preprint arXiv:2303.08774*.

Bai, S.; Chen, K.; Liu, X.; Wang, J.; Ge, W.; Song, S.; Dang, K.; Wang, P.; Wang, S.; Tang, J.; Zhong, H.; Zhu, Y.; Yang, M.; Li, Z.; Wan, J.; Wang, P.; Ding, W.; Fu, Z.; Xu, Y.; Ye, J.; Zhang, X.; Xie, T.; Cheng, Z.; Zhang, H.; Yang, Z.; Xu, H.; and Lin, J. 2025a. Qwen2.5-VL Technical Report. *arXiv:2502.13923*.

Bai, S.; Chen, K.; Liu, X.; Wang, J.; Ge, W.; Song, S.; Dang, K.; Wang, P.; Wang, S.; Tang, J.; et al. 2025b. Qwen2. 5-vl technical report. *arXiv preprint arXiv:2502.13923*.

Charpiat, G.; Girard, N.; Felardos, L.; and Tarabalka, Y. 2019. Input similarity from the neural network perspective. *Advances in Neural Information Processing Systems*, 32.

Chowdhury, P. N.; Sain, A.; Bhunia, A. K.; Xiang, T.; Gryaditskaya, Y.; and Song, Y.-Z. 2022. FS-COCO: Towards Understanding of Freehand Sketches of Common Objects in Context. In *ECCV*.

Deng, W.; Ren, Y.; Li, M.; Sutherland, D. J.; Li, X.; and Thrampoulidis, C. 2025. On the Effect of Negative Gradient in Group Relative Deep Reinforcement Optimization. *arXiv preprint arXiv:2505.18830*.

Deng, W.; Thrampoulidis, C.; and Li, X. 2024. Unlocking the potential of prompt-tuning in bridging generalized and personalized federated learning. In *Proceedings of the IEEE/CVF Conference on Computer Vision and Pattern Recognition*, 6087–6097.

Deng, W.; Zhong, Y.; Dou, Q.; and Li, X. 2023. On fairness of medical image classification with multiple sensitive attributes via learning orthogonal representations. In *International Conference on Information Processing in Medical Imaging*, 158–169. Springer.

Dettmers, T.; Pagnoni, A.; Holtzman, A.; and Zettlemoyer, L. 2023. Qlora: Efficient finetuning of quantized llms. *Advances in neural information processing systems*, 36: 10088–10115.

Ferrara, E. 2023. Should chatgpt be biased? challenges and risks of bias in large language models. *arXiv preprint arXiv:2304.03738*.

Ghorbani, A.; and Zou, J. 2019. Data shapley: Equitable valuation of data for machine learning. In *International conference on machine learning*, 2242–2251. PMLR.

Grosse, R.; Bae, J.; Anil, C.; Elhage, N.; Tamkin, A.; Tajdini, A.; Steiner, B.; Li, D.; Durmus, E.; Perez, E.; et al. 2023. Studying large language model generalization with influence functions. *arXiv preprint arXiv:2308.03296*.

Guo, D.; Yang, D.; Zhang, H.; Song, J.; Zhang, R.; Xu, R.; Zhu, Q.; Ma, S.; Wang, P.; Bi, X.; et al. 2025. Deepseek-r1: Incentivizing reasoning capability in llms via reinforcement learning. *arXiv preprint arXiv:2501.12948*.

Hao, Y.; Gu, J.; Wang, H. W.; Li, L.; Yang, Z.; Wang, L.; and Cheng, Y. 2025. Can MLLMs Reason in Multimodality? EMMA: An Enhanced MultiModal ReAsoning Benchmark. *arXiv preprint arXiv:2501.05444*.

Jaech, A.; Kalai, A.; Lerer, A.; Richardson, A.; El-Kishky, A.; Low, A.; Helyar, A.; Madry, A.; Beutel, A.; Carney, A.; et al. 2024. Openai o1 system card. *arXiv preprint arXiv:2412.16720*.

Jainr3. 2023. Jainr3/diffusiondb-pixelart · Datasets at Hugging Face. <https://huggingface.co/datasets/jainr3/diffusiondb-pixelart>. [Accessed 24-09-2023].

Koh, P. W.; and Liang, P. 2017. Understanding black-box predictions via influence functions. In *International conference on machine learning*, 1885–1894. PMLR.

Kong, S.; Shen, Y.; and Huang, L. 2021. Resolving training biases via influence-based data relabeling. In *International Conference on Learning Representations*.

Kwon, Y.; Wu, E.; Wu, K.; and Zou, J. 2024. Datainf: Efficiently estimating data influence in lora-tuned llms and diffusion models. *International Conference on Learning Representations*.

Meta, A. 2024. Llama 3.2: Revolutionizing edge AI and vision with open, customizable models. *Meta AI Blog*. Retrieved December, 20: 2024.

Mixon, D. G.; Parshall, H.; and Pi, J. 2022. Neural collapse with unconstrained features. *Sampling Theory, Signal Processing, and Data Analysis*, 20(2): 11.

Norod78. 2023. Norod78/cartoon-blip-captions · Datasets at Hugging Face. <https://huggingface.co/datasets/Norod78/cartoon-blip-captions>. [Accessed 24-09-2023].

Pruthi, G.; Liu, F.; Kale, S.; and Sundararajan, M. 2020. Estimating training data influence by tracing gradient descent. *Advances in Neural Information Processing Systems*, 33: 19920–19930.

Qwen; ; Yang, A.; Yang, B.; Zhang, B.; Hui, B.; Zheng, B.; Yu, B.; Li, C.; Liu, D.; Huang, F.; Wei, H.; Lin, H.; Yang, J.; Tu, J.; Zhang, J.; Yang, J.; Yang, J.; Zhou, J.; Lin, J.; Dang, K.; Lu, K.; Bao, K.; Yang, K.; Yu, L.; Li, M.; Xue, M.; Zhang, P.; Zhu, Q.; Men, R.; Lin, R.; Li, T.; Tang, T.; Xia, T.; Ren, X.; Ren, X.; Fan, Y.; Su, Y.; Zhang, Y.; Wan, Y.; Liu, Y.; Cui, Z.; Zhang, Z.; and Qiu, Z. 2025. Qwen2.5 Technical Report. *arXiv:2412.15115*.

Ruiz, N.; Li, Y.; Jampani, V.; Pritch, Y.; Rubinstein, M.; and Aberman, K. 2023. Dreambooth: Fine tuning text-to-image diffusion models for subject-driven generation. In *Proceedings of the IEEE/CVF conference on computer vision and pattern recognition*, 22500–22510.

Shao, Z.; Wang, P.; Zhu, Q.; Xu, R.; Song, J.; Bi, X.; Zhang, H.; Zhang, M.; Li, Y.; Wu, Y.; et al. 2024. Deepseekmath: Pushing the limits of mathematical reasoning in open language models. *arXiv preprint arXiv:2402.03300*.

Touvron, H.; Martin, L.; Stone, K.; Albert, P.; Almahairi, A.; Babaei, Y.; Bashlykov, N.; Batra, S.; Bhargava, P.; Bhosale, S.; et al. 2023. Llama 2: Open foundation and fine-tuned chat models. *arXiv preprint arXiv:2307.09288*.

Wang, J. T.; Mittal, P.; Song, D.; and Jia, R. 2024. Data shapley in one training run. *arXiv preprint arXiv:2406.11011*.

Wu, J.; Deng, W.; Li, X.; Liu, S.; Mi, T.; Peng, Y.; Xu, Z.; Liu, Y.; Cho, H.; Choi, C.-I.; et al. 2025. Medreason: Eliciting factual medical reasoning steps in llms via knowledge graphs. *arXiv preprint arXiv:2504.00993*.

Yang, J.; Deng, W.; Liu, B.; Huang, Y.; Zou, J.; and Li, X. 2025. Gmvaluator: Similarity-based data valuation for generative models. *International Conference on Learning Representations*.

Yang, Z.; Li, L.; Lin, K.; Wang, J.; Lin, C.-C.; Liu, Z.; and Wang, L. 2023. The dawn of Imms: Preliminary explorations with gpt-4v (ision). *arXiv preprint arXiv:2309.17421*, 9(1): 1.

Zhao, Y.; Behnia, T.; Vakilian, V.; and Thrampoulidis, C. 2024. Implicit geometry of next-token prediction: From language sparsity patterns to model representations. *arXiv preprint arXiv:2408.15417*.

Zhou, X.; Fan, S.; and Jaggi, M. 2024. HyperINF: Unleashing the HyperPower of the Schulz’s Method for Data Influence Estimation. *arXiv preprint arXiv:2410.05090*.

Zoheb. 2023. zoheb/sketch-scene · Datasets at Hugging Face. <https://huggingface.co/datasets/zoheb/sketch-scene>. [Accessed 24-09-2023].

8 Appendix

8.1 Training loss of LLMs and VLMs

To adapt a pretrained LLM or VLM to a specific domain or task, models are typically trained on a supervised dataset $\mathcal{D} = (\mathbf{x}_i, \mathbf{y}_i)_{i=1}^n$ of input-output pairs. Training is commonly performed using the standard teacher-forcing objective, which minimizes the negative log-likelihood of the target sequence:

$$\begin{aligned}\mathcal{L}_{\text{SFT}}(\theta) &= -\frac{1}{n} \sum_{i=1}^n \ln \pi_\theta(\mathbf{y}_i | \mathbf{x}_i) \\ &= -\frac{1}{n} \sum_{i=1}^n \sum_{k=1}^{|\mathbf{y}_i|} \ln \pi_\theta(y_{i,k} | \mathbf{x}_i, \mathbf{y}_{i,<k}).\end{aligned}$$

This objective maximizes the likelihood that the model generates the correct output sequence conditioned on the input and the ground-truth prefix at each step. The parameters are updated using gradient descent or its variants:

$$\theta \leftarrow \theta - \eta \nabla_\theta \mathcal{L}_{\text{SFT}}(\theta), \quad \text{with } \theta_{t=0} = \theta_0,$$

where $\eta > 0$ is the learning rate. Teacher forcing stabilizes fine-tuning by supplying the true prefix $\mathbf{y}_{<k}$ during training, enabling the model to align its predictions closely with the target data distribution in the new domain.

8.2 Proof of Theorem 1

In this section, we give the detailed proof of our Theorem 1, we start by proving the following theorem:

Theorem 2. *For a data \mathbf{x}_v and its generation \mathbf{y}_v that await valuation, at any time $t \geq 0$ of training using a training data $(\mathbf{x}_i, \mathbf{y}_i), i \in [n]$, in addition to the dependence on token unembeddings, the training data exhibits larger value to the valuation data as the following increases:*

$$\sum_{k=1}^{|\mathbf{y}_v|} \sum_{k'=1}^{|\mathbf{y}_i|} \alpha_{k,k'}(t) \cdot \left\langle \mathbf{h}_{\mathbf{x}_v, \mathbf{y}_{v,<k}}(t), \mathbf{h}_{\mathbf{x}_i, \mathbf{y}_{i,<k'}}(t) \right\rangle \quad (3)$$

Proof.

$$\begin{aligned}\frac{d}{dt} \ln \pi_{\theta(t)}(\mathbf{y}_v | \mathbf{x}_v) &= \left\langle \nabla \ln \pi_{\theta(t)}(\mathbf{y}_v | \mathbf{x}_v), \frac{d}{dt} \theta(t) \right\rangle \\ &= \left\langle \nabla \ln \pi_{\theta(t)}(\mathbf{y}_v | \mathbf{x}_v), -\eta \nabla \mathcal{L}_D(\theta) \right\rangle \\ &= \left\langle \nabla \ln \pi_{\theta(t)}(\mathbf{y}_v | \mathbf{x}_v), \eta \sum_{i=1}^n \nabla \ln \pi_{\theta(t)}(y_i | \mathbf{x}_i) \right\rangle\end{aligned}$$

As per the unconstrained features Assumption, the model's trainable parameters are

$$\theta = \left(\mathbf{W}, \mathbf{h}_{\mathbf{x}_v}, \{ \mathbf{h}_{\mathbf{x}_v, \mathbf{y}_{v,<k}} \}_{k \in \{2, \dots, |\mathbf{y}_v|\}}, \{ \mathbf{h}_{\mathbf{x}_i, \mathbf{y}_{i,<k'}} \}_{i \in [n], k' \in \{1, \dots, |\mathbf{y}_i|\}} \right).$$

Unfolding the gradients with respect to these parameters yields:

$$\begin{aligned}\frac{d}{dt} \ln \pi_{\theta(t)}(\mathbf{y}_v | \mathbf{x}_v) &= \left\langle \nabla_{\mathbf{W}} \ln \pi_{\theta(t)}(\mathbf{y}_v | \mathbf{x}_v), \sum_i^n \nabla_{\mathbf{W}} \ln \pi_{\theta(t)}(y_i | \mathbf{x}_i) \right\rangle \\ &\quad + \underbrace{\sum_{k=1}^{|\mathbf{y}_v|} \left\langle \nabla_{\mathbf{h}_{\mathbf{x}_v, \mathbf{y}_{v,<k}}} \ln \pi_{\theta(t)}(\mathbf{y}_{v,k} | \mathbf{x}_v, \mathbf{y}_{v,<k}), \sum_{i'=1}^{n_k} \nabla_{\mathbf{h}_{\mathbf{x}_v, \mathbf{y}_{v,<k}}} \ln \pi_{\theta(t)}(y_{i',k} | \mathbf{y}_{v,<k}) \right\rangle}_{\text{(II) Training data have the same } (\mathbf{x}_v, \mathbf{y}_{v,<k})}.\end{aligned} \quad (4)$$

where n_k is the number of training data whose input and prediction before token k are the same as valuation data $(\mathbf{x}_v, \mathbf{y}_{v,<k})$. Since we have

$$\begin{aligned}\nabla_{\mathbf{W}} \ln \pi_{\theta(t)}(z | \mathbf{x}) &= \left(\mathbf{e}_z - \sum_{z' \in \mathcal{V}} \pi_{\theta(t)}(z' | \mathbf{x}) \cdot \mathbf{e}_{z'} \right) \mathbf{h}_{\mathbf{x}}^\top(t), \\ \nabla_{\mathbf{h}_{\mathbf{x}}} \ln \pi_{\theta(t)}(z | \mathbf{x}) &= \mathbf{W}_z(t) - \sum_{z' \in \mathcal{V}} \pi_{\theta(t)}(z' | \mathbf{x}) \cdot \mathbf{W}_{z'}(t).\end{aligned}$$

Putting this back in (4) together with a few algebra steps, yields

$$\frac{d}{dt} \ln \pi_{\theta(t)}(\mathbf{y}_v | \mathbf{x}_v) = (\text{I}) + (\text{II}) \quad (5)$$

where:

$$(\text{I}) = \sum_{k=1}^{|\mathbf{y}_v|} \sum_{i=1}^n \sum_{k'=1}^{|\mathbf{y}_i|} \alpha_{k,k'}(t) \cdot \left\langle \mathbf{h}_{\mathbf{x}_v, \mathbf{y}_{v, < k}}(t), \mathbf{h}_{\mathbf{x}_i, \mathbf{y}_{i, < k'}}(t) \right\rangle \quad (6)$$

$$(\text{II}) = \sum_{k=1}^{|\mathbf{y}_v|} \left\langle \mathbf{w}_{\mathbf{y}_{v,k}}(t) - \sum_{z \in \mathcal{V}} \pi_{\theta(t)}(z | \mathbf{x}_v) \cdot \mathbf{w}_z(t), \sum_{i'=1}^{n_k} (\mathbf{w}_{\mathbf{y}_{i',k}} - \sum_{z \in \mathcal{V}} \pi_{\theta(t)}(z | \mathbf{x}_v) \cdot \mathbf{w}_z(t)) \right\rangle \quad (7)$$

where $\alpha_{k,k'}(t) = \left\langle \mathbf{e}_{\mathbf{y}_{v,k}} - \pi_{\theta(t)}(\cdot | \mathbf{x}, \mathbf{y}_{v, < k}), \mathbf{e}_{\mathbf{y}_{i,k'}} - \pi_{\theta(t)}(\cdot | \mathbf{x}, \mathbf{y}_{i, < k'}) \right\rangle$. Thus we can obtain the theorem. \square

We observe the following:

(1) When the training input \mathbf{x}_i differs from the valuation input \mathbf{x}_v , its influence on the valuation target arises solely through Term (I), which captures the contribution of the token embeddings and all network parameters except the token unembedding layer.

(2) The effect of the token unembeddings is concentrated in cases where the training and valuation data share the same input \mathbf{x} and exhibit overlapping output predictions \mathbf{y} .

To eliminate this dependence on token unembeddings, we impose the following assumption:

Assumption 2 (Distinct Input). *The training dataset satisfies that no training input \mathbf{x}_i is identical to the valuation input \mathbf{x}_v .*

Under the Assumption 2, the contribution from token unembeddings (Term (II)) vanishes, so that the influence of the training data on the valuation data arises entirely through the shared representation features captured in Term (I). This assumption is mild, as training inputs typically differ from valuation inputs in practice — especially in vision-language datasets, where the input images are almost always distinct. Extending this result to cases where training examples share the same input but differ in their outputs \mathbf{y} is straightforward: the output prefix $\mathbf{y}_{< k}$ can be incorporated into the input \mathbf{x} , treating each unique pair $(\mathbf{x}, \mathbf{y}_{< k})$ as a distinct input, where $k - 1$ indicates the point at which the outputs begin to differ. Combining Theorem 2 and Assumption 2 then yields Theorem 1.

8.3 Detailed Task Description

LLM Influence Evaluation Tasks Following (Kwon et al. 2024), we evaluate the performance of For-Value on three text generation tasks for large language models (LLMs) to identify influential data points:

- **Sentence Transformations:** This task requires transforming input sentences into alternative forms while preserving meaning (e.g., active to passive voice). The dataset comprises 10 distinct classes (e.g., declarative to interrogative), each with 100 examples, split into 90 training and 10 test examples per class. Data examples see Tab. 5.
- **Math Word Problems (Without Reasoning):** These problems involve direct numerical computation from textual descriptions (e.g., basic arithmetic). The dataset has 10 classes based on operation types, with 100 examples per class (90 training, 10 test). Data examples see Tab. 6.
- **Math Word Problems (With Reasoning):** These require multi-step reasoning (e.g., solving word problems involving algebra or logic). Similar to the previous task, the dataset includes 10 classes with 100 examples each (90 training, 10). Data examples see Tab. 6.

VLM Influence Evaluation Tasks For VLMs, we adapt text-to-image generation tasks from (Kwon et al. 2024) into image-to-text (captioning) tasks to evaluate influence:

- **Style Generation:** This task involves generating captions for images in specific styles: cartoons (Norod78 2023), pixel art (Jainr3 2023), and line sketches (Zoheb 2023). Each style dataset contains 200 training and 50 test image-text pairs, totaling 600 training and 150 test samples across three styles. Data examples see Fig. 3.
- **Subject Generation:** Using the DreamBooth dataset (Ruiz et al. 2023), this task generates captions for images of 30 distinct subjects (e.g., specific objects or animals). Each subject provides 3 training samples, with the remaining samples used for validation. Data examples see Fig. 3.

Influential Data Detection Metrics We adopt two metrics from (Kwon et al. 2024) to assess influence:

- **AUC Score:** For each test data point, we assign pseudo labels to training points (1 if the training point's label matches the test point's, 0 otherwise). We compute the Area Under the Curve (AUC) between data values (influence scores) and pseudo labels, averaging across all test points. A higher AUC indicates better identification of influential points.
- **Recall:** For each test point, we calculate the percentage of influential training points (top-ranked by influence score) that share the same class as the test point. This measures the relevance of identified influential points.

Mislabeled Data Detection Data & Metrics For mislabeled detection, we transform the dataset into a visual-language question answering task with the template "What is the animal in the image? It is a [label]" with demonstration³ in Fig. 5. We then select the first 400 images for both dogs and cats, flipping 50% of the labels to introduce noise. For validation, we use 200 images, with each class containing 100 images. For evaluation, we also calculate the AUC and Recall but with the pseudo labels to training points being 1 if the training point's label matches the test point's and 0 otherwise.

Baseline Selection For baseline methods, we select the model checkpoint with the highest test AUC, as influence function-based methods exhibit significant performance variability across training checkpoints. Notably, this variability does not correlate with validation loss, posing challenges for practical deployment. We compare `For-Value` against these baselines to ensure robust evaluation.

Table 4: Dataset statistics for LLM and VLM tasks.

Task	Training Samples	Test/Validation Samples
Sentence Transformations	900 (90 × 10 classes)	100 (10 × 10 classes)
Math Word Problems (No Reasoning)	900 (90 × 10 classes)	100 (10 × 10 classes)
Math Word Problems (With Reasoning)	900 (90 × 10 classes)	100 (10 × 10 classes)
Style Generation	600 (200 × 3 styles)	150 (50 × 3 styles)
Subject Generation	90 (3 × 30 subjects)	Variable (1-3) per subject
Mislabel Detection	800 (400 × 2 subjects 50% noise)	200 (100 × 2 subjects)

Dataset Statistics

8.4 Additional Details

Training setting for baselines. While `For-Value` requires only a single forward pass, the influence function-based baselines `Hessian-free` and `DataInf` require fine-tuning the models to convergence. For text generation tasks, we follow the training setup in (Kwon et al. 2024), except to llama-2-13B, we use float16 weights instead of 8-bit quantization. For image-to-text generation tasks, we apply LoRA to every query and value matrix within the model’s attention layers. To finetune VLMs, we use a learning rate of 2×10^{-4} , LoRA hyperparameters $r = 8$ and $\alpha = 32$, float16 model weights, a batch size of 32, and train for 20 epochs.

Table 5: Description of the sentence transformation task templates. We consider 10 different types of sentence transformations. For each sentence transformation, unique identifying “chatbot” names were additionally prepended to the task prompt to assist the model in training.

Sentence transformations	Example transformation of “Sunrises herald hopeful tomorrows”:
Reverse Order of Words	tomorrows. hopeful herald Sunrises
Capitalize Every Other Letter	sUnRiSeS hErAID hOpEfUl tOmOrRoWs.
Insert Number 1 Between Every Word	Sunrises 1herald 1hopeful 1tomorrows.
Replace Vowels with *	S*nr*s*s h*r*ld h*p*f*l t*m*rr*ws.
Double Every Consonant	SSunrriisseess hheraldd hhopefull ttomorrows.
Capitalize Every Word	Sunrises Herald Hopeful Tomorrows.
Remove All Vowels	Snrss hrld hpf1 tmrrws.
Add 'ly' To End of Each Word	Sunrisesly heraldly hopefully tomorrows.ly
Remove All Consonants	uie ea oeu ooo.
Repeat Each Word Twice	Sunrises Sunrises herald herald hopeful hopeful tomorrows. tomorrows.

8.5 License Clarification

The Dreambooth images have been either taken by the authors of the paper or obtained from Unsplash⁴. The file located at this link⁵ includes a list of all reference links to the images on Unsplash, along with the photographers’ attributions and the image

³To prevent any licensing issues, the images shown are not from the original dataset; they were personally captured for demonstration purposes.

⁴<https://www.unsplash.com/>

⁵https://huggingface.co/datasets/google/dreambooth/blob/main/dataset/references_and_licenses.txt

Table 6: Description of the math problem task templates. We consider 10 different types of math word problems.

Math Word Problems	Template prompt question
Remaining pizza slices	Lisa ate A slices of pizza and her brother ate B slices from a pizza that originally had C slices. How many slices of the pizza are left? Reason: Combined slices eaten = A + B. Left = C - (A + B).
Chaperones needed for trip	For every A students going on a field trip, there are B adults needed as chaperones. If C students are attending, how many adults are needed? Reason: Adults needed = (B * C) // A.
Total number after purchase	In an aquarium, there are A sharks and B dolphins. If they bought C more sharks, how many sharks would be there in total? Reason: Total sharks = A + C.
Total game points	Michael scored A points in the first game, B points in the second, C in the third, and D in the fourth game. What is his total points? Reason: Total points = A + B + C + D.
Total reading hours	Emily reads for A hours each day. How many hours does she read in total in B days? Reason: Total hours read = A * B.
Shirt cost after discount	A shirt costs A. There's a B-dollar off sale. How much does the shirt cost after the discount? Reason: Cost after discount = A - B.
Area of a garden	A rectangular garden has a length of A meters and a width of B meters. What is its area? Reason: Area = A * B.
Total savings	If Jake saves A each week, how much will he save after B weeks? Reason: Total savings = A * B.
Number of cupcake boxes	A bakery sells cupcakes in boxes of A. If they have B cupcakes, how many boxes can they fill? Reason: Boxes filled = B // A.
Interest earned	John invests A at an annual interest rate of B%. How much interest will he earn after C years? Reason: Interest = (A * B * C) // 100.

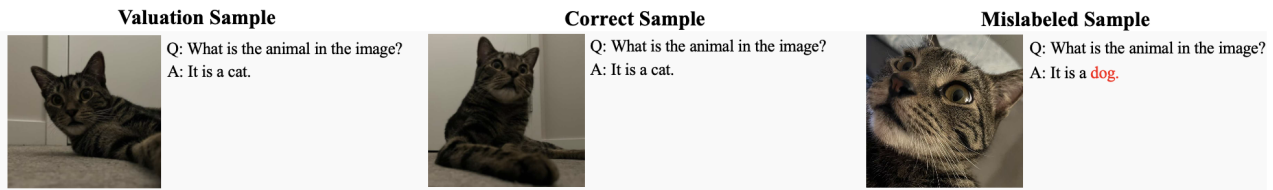


Figure 5: Description of the mislabeled data detection task. We utilize a cat versus dog classification dataset and intentionally introduce noise by randomly swapping the labels of 50% of the data.

licenses. The sketch images are sourced from FS-COCO (Chowdhury et al. 2022). Data attributions and image licenses can be found in the file provided at the following link⁶.

⁶<https://github.com/pinakinathc/fscoco>